









## Spatial-temporal dynamics of the Caatinga vegetation cover by remote sensing in municipality of the Brazilian semi-arid

Jhon Lennon Bezerra da Silva<sup>1</sup>, Geber Barbosa de Albuquerque Moura<sup>1</sup>, Ênio Farias de França e Silva<sup>1</sup>,  
Fabrício Marcos Oliveira Lopes<sup>1</sup>, Tecla Ticiane Félix da Silva<sup>1</sup>, Frederico Abraão Costa Lins<sup>1</sup>,  
Douglas Alberto de Oliveira Silva<sup>1</sup>, Pedro Francisco Sanguino Ortiz<sup>1</sup>

<sup>1</sup> Universidade Federal Rural de Pernambuco, Recife-PE, Brasil. E-mail: jhonlennoigt@hotmail.com; geber.moura@ufrpe.br; enio.fsilva@ufrpe.br; fabrício.lopez@ufrpe.br; teclaticiane12@hotmail.com; frederico\_acl@hotmail.com; douglasalbertosilva@hotmail.com; francisko369@gmail.com

**ABSTRACT:** The aim of this study was to monitor and evaluate the Caatinga vegetation cover in a municipality from the Brazilian semi-arid through of the spatial-temporal distribution of vegetation indexes by remote sensing. The study was developed using six satellite images which covers the municipality of Iguatu, Ceará. Thematic maps of the SAVI and LAI vegetation indexes were developed and evaluated by descriptive statistics and according to their spatial-temporal variability. Maps of the SAVI and LAI showed high heterogeneity in the spatial-temporal distribution pattern, classified as medium variability (CV = 35 to 57%) and high variability (CV = 63 to 104%), respectively. The indexes provided answers as to the land uses behavior pattern, highlighting conditions of changes in the Caatinga vegetation. In general, the SAVI and LAI indexes showed a low condition of the vegetal biomass over time, a typical spatial-temporal dynamics characteristic in the dry season of the semi-arid. The vegetation indexes detected a remarkable sensitivity of the Caatinga vegetation to the presence and/or absence of rainfall, owing a high resilience capacity in response to intense rainfall. The semi-arid region becomes more vulnerable due to the intensification of drought events.

**Key words:** deforestation; drought; environmental degradation; IAF; SAVI

## Dinâmica espaço-temporal da cobertura vegetal de Caatinga por sensoriamento remoto em município do semiárido brasileiro

**RESUMO:** Objetivou-se monitorar e avaliar a cobertura vegetal de Caatinga em município do semiárido brasileiro através da distribuição espaço-temporal de índices de vegetação por sensoriamento remoto. O estudo foi desenvolvido utilizando-se seis imagens de satélite que cobrem o município de Iguatu, Ceará. Foram desenvolvidos mapas temáticos dos índices de vegetação SAVI e IAF, avaliados pela estatística descritiva e quanto sua variabilidade espaço-temporal. Os mapas do SAVI e IAF apresentaram alta heterogeneidade no padrão de distribuição espaço-temporal, classificados como de média variabilidade (CV = 35 a 57%) e alta variabilidade (CV = 63 a 104%), respectivamente. Os índices originaram respostas do padrão de comportamento dos usos do solo, destacando condições de mudanças na vegetação de Caatinga. O SAVI e IAF destacaram baixa condição da biomassa vegetal ao longo do tempo, dinâmica espaço-temporal característica na estação seca do semiárido. Os índices de vegetação detectaram sensibilidade da vegetação de Caatinga à presença e/ou ausência de chuva, tendo alto poder de resiliência em respostas as maiores precipitações. A região semiárida encontra-se mais vulnerável devido à intensificação dos eventos de seca.

**Palavras-chave:** desmatamento; seca; degradação ambiental; IAF; SAVI

## Introduction

A lack of observation and environmental monitoring, both in space and time, is a constant in the semi-arid regions of Brazil. It is essential to look for efficient tools, methods and technologies to meet needs, such as the absence of environmental data in hard to reach areas, which makes it impossible to understand the anthropic actions that expand areas of exposed soil in the semi-arid, such as deforestation and burning. The natural Caatinga vegetation of these environments is constantly degraded by anthropic activities, with these being mainly potentiated by severe droughts, which in turn promote severe water deficit, low humidity and temperature increase, consequently favoring the desertification process in the semi-arid (Gutiérrez et al., 2014; Marengo et al., 2016; Mariano et al., 2018).

In the last decades, geotechnology has been prominent in the geotechnologies development and has opened a new area of action for environmental monitoring of semi-arid regions from Brazil and the world, in particular the technologies involved in the detection of spectral responses in airborne and orbital sensors, part of the scope of remote sensing. Among the most used applications in this segment, the studies on detection, analysis and monitoring of the Caatinga biome vegetation cover stand out (Silva & Galvêncio, 2012; Vieira et al., 2013; Bezerra et al., 2014; Vieira et al., 2015; Lins et al., 2017; Oliveira et al., 2017; Barbosa et al., 2018; Campos et al., 2019).

Remote sensing has great advantage in monitoring large-scale areas in space and time, at a more affordable cost-benefit ratio and, when coupled with area meteorological and morphological information, enables the obtaining of reliable results. Among the performed analyzes with this technology, the applications of vegetation indexes are important to distinguish the spectral information of the vegetation from other elements of the terrestrial surface, in addition of indicating the quantity and quality of the observed vegetation. In particular, the Soil Adjusted Vegetation Index (SAVI), a biophysical parameter that seeks to attenuate the previous effects of the soil, correcting it by the adjustment factor limitations imposed by other indexes in the semi-arid; and also the leaf area index (LAI), important in highlighting in Caatinga vegetation the highest/lowest photosynthetic activity, thus indicating the quality of plant biomass. Based on this information, it is possible proposing appropriate management and guiding the exploitation of plant resources (Allen et al., 2007; Silva & Galvêncio, 2012; Ribeiro et al., 2016; Leite et al., 2017; Lins et al., 2017; Oliveira et al., 2017).

Given the above, this study aimed to monitor and evaluate the natural vegetation dynamics of Caatinga from the spatial-temporal modeling of vegetation indexes by remote sensing means, using satellite images for the municipality of Iguatu-CE, Brazilian semi-arid, in order to highlight the major changes in the earth surface due to drought events and anthropic activities between 2008 and 2015.

## Materials and Methods

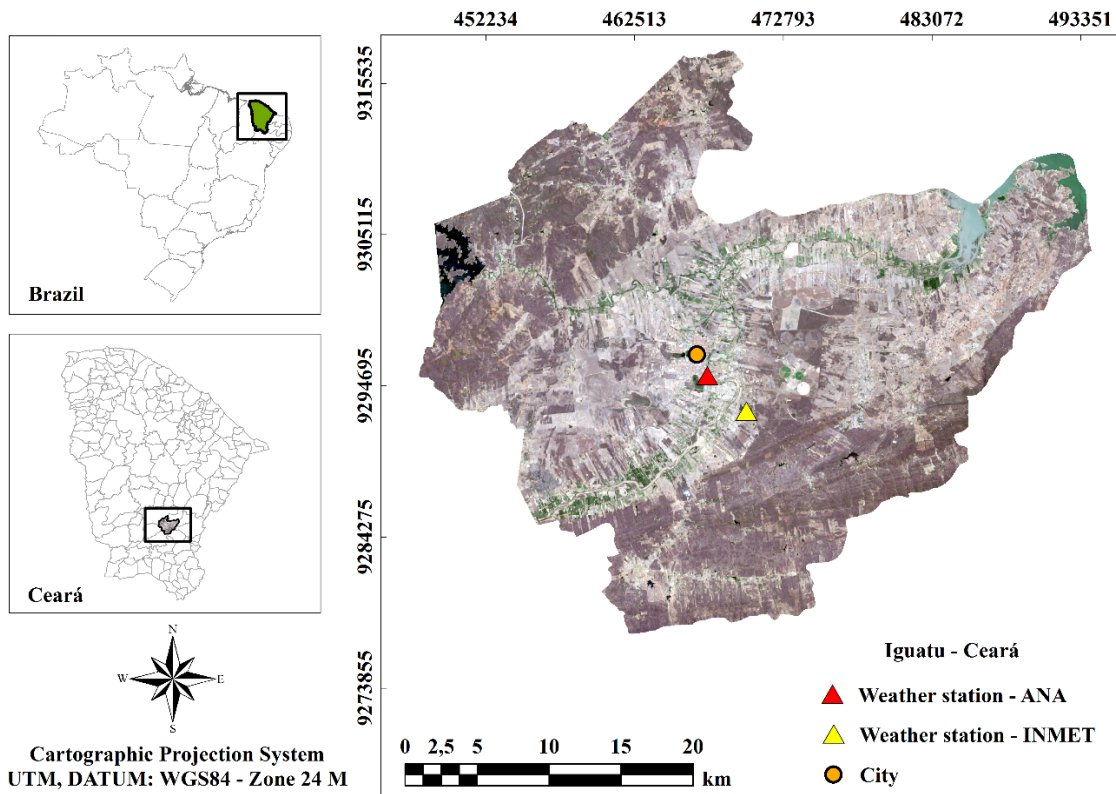
The study area, municipality of Iguatu, is located in the state of Ceará, semi-arid region from the Northeastern Brazil, located between the parallels of 06°11'31.78"S (UTM: 9315534 m) and 06°34'9.76"S (UTM: 9273854 m), and between the meridians of 39°3'36.52"W (UTM: 493351 m) and 39°25'54.33"W (UTM: 452234 m), at an elevation of 217.8 m to the west of the Greenwich meridian. According to Köppen classification, the region has a BSw'h' climate characterization (hot and semi-arid climate). The region has an absolute surface area of 1,029 km<sup>2</sup>, characterized by the predominance of Caatinga vegetation, with an mean annual air temperature of 26 to 28 °C, and an mean annual precipitation of 817.91 mm (historical series of 30 years of climatological data, among 1989 and 2018, recorded by the rainfall station from National Water Agency (ANA), code: 00639044, at the coordinates of 06°22'27.4"S (UTM: 9295412 m) and 39°17'35.9"W (UTM: 467563 m), zone 24 S (24 M zone) with irregular rainfall in both time and space. It has two well-defined seasons during the year, one rainy and the other dry. The rainy season is between the months of January and April. The dry season can last from 7 to 8 months and shows high temperatures that cause high evaporation rates (Alvares et al., 2013; IPECE, 2017).

Figure 1 displays the spatial map of the study area location, municipality of Iguatu-CE, through a Landsat-8 satellite image, OLI sensor (Operational Land Imager), acquired on 08/24/2015, in R4G3B2 composition, natural color. Highlighted on it are the weather stations responsible for the surface data and the location point of the city. Green-hued pixels highlight areas of irrigated agriculture in the region, related to the crops of corn, beans, bananas, cassava, rice, among other subsistence agriculture crops that control local socioeconomic conditions. The image was georeferenced by the Universal Transverse Mercator Map Projection System (UTM), DATUM: WGS84, zone 24 M.

Table 1 displays the accumulated rainfall records from the previous 30 days and also from the trimester prior to the satellite passages in the study area and the annual total.

The research was developed by using six satellite images, three from Landsat-5, TM sensor (Thematic Mapper) for 09/21/2008, 06/20/2009, 08/29/2011, and three from Landsat-8, Operational Land Imager sensor (OLI) for the days of 03/09/2013, 09/22/2014 and 08/24/2015. Spatial resolution from the multispectral bands of the satellite images is of 30 m; 8-bit radiometric resolution for the TM sensor and 12-bit for the OLI sensor. Images were made available by the North American National Aeronautics and Space Administration (NASA) space agency via image acquisition through the United States Geological Survey (USGS) website. The main selection criteria were: absence of clouds and the periodicity of the images, which these having been collected during the dry season of the year.

Digital image processing was performed by using the ERDAS IMAGINE® 9.1 software, with some steps from Surface Energy Balance Algorithms for Land (SEBAL) (Bastiaanssen,



**Figure 1.** Spatial location of the municipality of Iguatu, Ceará, Brazil.

**Table 1.** Records of the previous accumulated precipitations prior to the satellites passage.

Date	Accumulated precipitation (mm)		
	Previous 30 days	Previous trimester	Annual total
09/21//2008	4.8	30.2	1,392.8
06/20//2009	26.0	516.2	1,079.2
08/29//2011	10.6	125.5	1,335.6
09/03//2013	6.4	149.0	649.8
09/22//2014	8.2	58.8	867.2
08/24//2015	2.8	34.0	526.2

Source: INMET (2019).

2000; Allen et al., 2002). The multispectral bands of the images were stacked and georeferenced by using the DATUM UTM (Universal Transverse Mercator) Map Projection System: WGS84, 24M Zone, in which the study area is located. Gray levels of the satellite images have been converted to spectral radiance and monochromatic reflectance by means of mathematical modeling and operations. Thus, using the reflective bands, the soil adjusted vegetation index (SAVI) and the leaf area index (LAI) were determined.

Spectral radiance represents the solar energy reflected by each pixel of the images per unit area, time, solid angle

and wavelength, measured for the Landsat-5 TM satellite with respect to the multispectral bands 3 (red) and 4 (near-IR) (Table 2); and Landsat-8 OLI for multispectral bands 4 (red band; wavelength between 0.630 and 0.680 [ $\mu\text{m}$ ]) and 5 (near infrared band; wavelength between 0.845 and 0.885 [ $\mu\text{m}$ ]).

The process of converting gray levels to the spectral radiance and monochrome reflectance of the Landsat-5 TM satellite used calibration coefficients, represented by the minimum ( $L_{\min}$ ) and maximum ( $L_{\max}$ ) radiance coefficients, regarding the period after April 2007 for each band (red; infrared: medium-IR), which is the period related to the images of this study; in addition to the spectral solar irradiance ( $k_{b \text{ Landsat } 5}$ ) of each of the Landsat-5 TM bands used at the top of the atmosphere (Table 2).

Spectral radiance in each Landsat-5 TM band was determined according to Equation 1 (Chander et al., 2009).

$$L_{b \text{ Landsat } 5} = L_{\min b} + \left( \frac{L_{\max b} - L_{\min b}}{255} \right) \times (ND_b - 1) \quad (1)$$

in which  $L_{b \text{ Landsat } 5}$  ( $\text{W m}^{-2} \text{sr}^{-1} \mu\text{m}^{-1}$ ) is the spectral radiance of each pixel in each band from Landsat-5;  $b$  (underwritten) represents each of the satellite bands;  $L_{\min b}$  and  $L_{\max b}$  ( $\text{W m}^{-2}$

**Table 2.** Calibration coefficients for converting gray levels of satellite images into radiance and reflectance for Landsat-5 TM.

Band	Wave length ( $\mu\text{m}$ )	Calibration coefficient of Landsat-5, TM sensor ( $\text{W m}^{-2} \text{sr}^{-1} \mu\text{m}^{-1}$ )		Solar spectral irradiation ( $k_{b \text{ Landsat } 5}$ ) at the atmosphere top ( $\text{W m}^{-2} \mu\text{m}^{-1}$ )
		$L_{\min}$	$L_{\max}$	
3 (red)	0.63 – 0.69	-1.17	264	1536
4 (near-IR)	0.76 – 0.90	-1.51	221	1031

$sr^{-1} \mu m^{-1}$ ) are the minimum and maximum spectral radiances, respectively (Table 2);  $ND$  is the pixel intensity (digital number between 0 and 256 levels of gray).

Determination of the spectral radiance in the Landsat-8 OLI satellite images was performed through Equation 2 (Chander et al., 2009).

$$L_{b \text{ Land } 8} = Add_{rad} + Mult_{rad} \times ND_b \quad (2)$$

in which  $L_{b \text{ Land } 8}$  ( $W m^{-2} sr^{-1} \mu m^{-1}$ ) is the spectral radiance in each band of Landsat-8, based in the additive ( $Add_{rad}$ ) and multiplicative ( $Mult_{rad}$ ) terms regarding radiance;  $ND$  is the pixel intensity (digital number between 0 and 65,535 levels of gray, high image detailing level, ensuring more information from the study area).

From the radiance, the monochrome reflectance of the Landsat-5 TM satellite images was determined, based on the spectral solar irradiance at the top of the atmosphere ( $k_{b \text{ Land } 5}$ ), through Equation 3 (Chander et al., 2009).

$$r_{b \text{ Land } 5} = \frac{\pi \times L_{b \text{ Land } 5}}{k_{b \text{ Land } 5} \times \cos \theta \times d_r} \quad (3)$$

in which  $r_{b \text{ Land } 5}$  ( $W m^{-2} sr^{-1} \mu m^{-1}$ ) is the monochrome spectral reflectance in each band from Landsat-5 TM;  $\theta$  is the solar zenith angle obtained from the Sun elevation angle provided by NASA/USGS;  $d_r$  is the squared ratio between the mean and instantaneous distances between the earth and the sun on a given imaged day of the year.

Monochrome reflectance for Landsat-8 OLI was determined from the Equation 4 (Chander et al., 2009).

$$r_{b \text{ Land } 8} = \frac{(Add_{ref} + Mult_{ref} \times ND_b)}{\cos \theta \times d_r} \quad (4)$$

in which  $r_{b \text{ Land } 8}$  ( $W m^{-2} sr^{-1} \mu m^{-1}$ ) is the monochrome reflectance in each band of the Landsat-8 OLI, also based on the additive ( $Add_{ref}$ ) and multiplicative ( $Mult_{ref}$ ) terms, regarding reflectance.

The squared ratio between the mean and instantaneous distances between the earth and the sun was determined from the Equation 5 (Iqbal, 1983).

$$d_r = 1 + 0.033 \times \cos \left( \frac{SDY \times 2 \times \pi}{365} \right) \quad (5)$$

in which  $SDY$  is the sequential day of the year; and the  $\cos$  function argument in radians.

From the multispectral reflective bands of satellite images, the vegetation indexes were determined. The soil adjusted vegetation index (SAVI) was determined according to Equation 6 (Allen et al., 2002).

$$SAVI = \frac{(1+L) \times (r_{b \text{ IV}} - r_{b \text{ V}})}{(L + r_{b \text{ IV}} + r_{b \text{ V}})} \quad (6)$$

in which  $r_{b \text{ IV}}$  and  $r_{b \text{ V}}$  correspond to the reflective bands 4 and 3 from Landsat-5 TM sensor; and Landsat-8 bands 5 and 4, to OLI

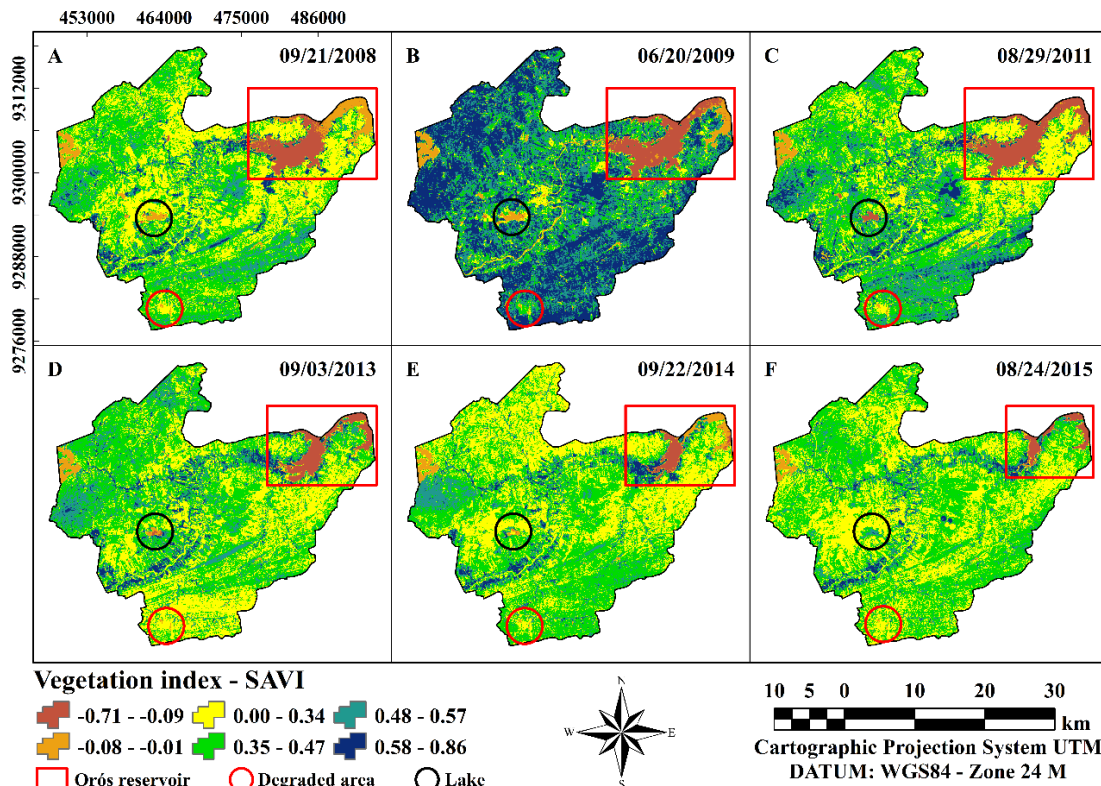


**Figure 2.** Spatial-temporal distribution monitoring of the SAVI vegetation index in the municipality of Iguatu-CE, semi-arid region of Northeastern Brazil.

sensor;  $L$  is the soil adjustment factor, which varies between 0 and 1, according to the vegetation cover density of the study area. An adjustment factor of 0.5 was used, which indicates an area with intermediate vegetation cover (Huete, 1988; Allen et al., 2007). The chosen factor refers to the study area, which is located in the Brazilian semi-arid and has Caatinga vegetation (Silva & Galvncio, 2012).

With the determination of the SAVI vegetation index, the leaf area index (LAI,  $m^2 m^{-2}$ ), an indicator of the biomass amount, was also determined from the Equation 7 (Allen et al., 2007).

$$LAI = -\frac{\ln\left(\frac{0.69 - SAVI}{0.59}\right)}{0.91} \quad (7)$$

Thematic maps of the vegetation indexes were developed aided by the ArcGIS<sup>®</sup> 10.2.2 software. In the software through reclassification techniques, a supervised thematic classification analysis of the SAVI and LAI vegetation indexes maps was held, highlighting the different land uses of the region, such as water bodies, exposed soil and urban area, irrigated areas and Caatinga, both thin and dense.

Land uses were divided into classes according to the appropriate range, where a careful analysis pixel-by-pixel in the vegetation indexes thematic maps was performed. Moreover, the values highlighted in the classes of the present study corroborate with studies conducted also in the semi-arid, which served as the basis and comparison of results.

The main results of the thematic maps were evaluated by descriptive statistics through measures of central tendency (mean, mode, median) and dispersion measures (minimum; maximum; standard deviation – SD; coefficient of variation – CV). Thematic maps were also evaluated for their spatial-temporal variability through the CV values (%), according to the classification criteria of Warrick & Nielsen (1980):  $CV < 12\%$  - low variability;  $12\% < CV < 60\%$  - medium variability and  $CV > 60\%$  - high variability.

## Results and Discussion

The thematic maps of SAVI and LAI vegetation indexes showed spatial-temporal behavior of medium variability (from 35 to 57%) and high variability (from 63 to 104%), respectively. The region has different land uses and occupations, with areas directed to agricultural activities, as well as reservoirs, rivers and lakes, thin and dense vegetation areas of Caatinga, and urban area.

Figure 2 displays the spatial-temporal distribution of the SAVI vegetation index from thematic maps of the surface between 2008 and 2015. SAVI seeks to mitigate the previous effects of the soil by means of an adjustment factor, and it is dependent on the soil type of the region, thus weighing limitations imposed by other indexes, especially in the Brazilian semi-arid regions (Huete, 1988; Ribeiro et al., 2016).

SAVI maps ranged from -0.71 to 0.86. In water bodies, negative SAVI values were found, ranging between -0.71 and -0.01 (red and burnt-yellow pixels). Areas of exposed and urban soil, as well as areas of undergrowth, had values between 0.00 and 0.34 (light-yellow pixels) (Figure 2). These values corroborate with the results obtained by Maranho et al. (2017), in which positive values close to zero and/or zero were obtained for exposed soil areas and urban perimeter, and negative values for water bodies. Areas of thin and dense Caatinga, with strong presence of moisture, and irrigated areas showed the highest SAVI values, between 0.35 and 0.86 (Figure 2).

Figure 3 displays the quantification of areas of the class intervals from SAVI vegetation index thematic maps for land use and soil occupation in the municipality of Iguatu-CE, semi-arid region of the Brazilian Northeastern.

Classes 1 and 2 correspond to the temporal distribution of areas covered by water bodies, which together had the highest percentages on 09/21/2008; 06/20/2009 and 08/29/2011, with values of 7.67% (78.86  $km^2$ ); 8.42% (86.56  $km^2$ ) and 7.46% (78.86  $km^2$ ) of the total area, respectively (Figure 3). According to the INMET records, the years in question had high precipitations, way above the historical mean of the municipality (817.91 mm), with the respective annual totals of 1,392.8; 1,079.2 and 1,335.6 mm (Table 1). During this period, the rains allowed the reservoirs to have a large water supply, although they did not reach their full capacity. However, the days of 03/09/2013; 09/22/2014 and 08/24/2015 refer to dates within the dry season in the semi-arid and had reduction in areas covered by water bodies, showing percentages of 4.38% (44.99  $km^2$ ); 3.33% (34.25  $km^2$ ) and 2.25% (23.10  $km^2$ ), respectively (Figure 3). According to INMET, in this period, the years had rains below the historical mean of the municipality, with the respective annual totals of 649.8; 867.2 and 526.2 mm (Table 1).

The severe effect of the drought can be evidenced by the decrease of the oros reservoir water mirror (northeastern region of the maps), evidenced by the red rectangle, and in

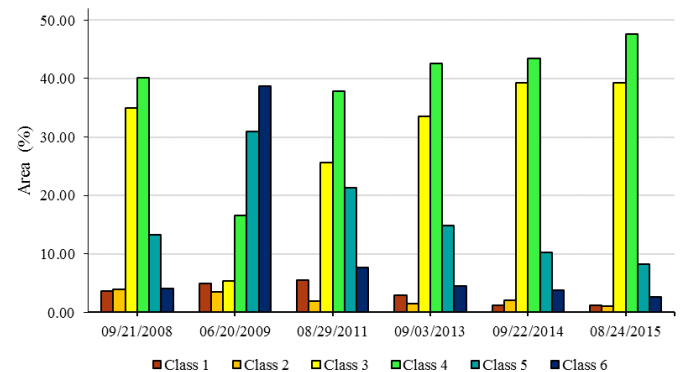


**Figure 3.** Quantification of SAVI thematic map class intervals in the different land uses and occupations of the semi-arid region. Class 1: between -0.71 and -0.09; Class 2: between -0.08 and -0.01; Class 3: between 0.00 and 0.34; Class 4: between 0.35 and 0.47; Class 5: between 0.48 and 0.57; Class 6: between 0.58 and 0.86.

a lake located in the southwest region of the municipality, highlighted by the black circle (Figure 2), which has been totally suppressed over time, as can be seen on the map on 08/24/2015 (Figure 2F), having been replaced by vegetation.

Drought was strongly installed in the semi-arid region of Brazil, especially in the state of Ceará, between 2012 and 2016, mainly affecting the water availability of reservoirs, causing high water deficit, with large losses, especially in the subsistence agriculture of the regions (Gutiérrez et al., 2014; Barbosa et al., 2018; Marengo et al., 2018).

Figure 4 displays the behavior of the water condition over time, that is, the quantification of the areas covered by water bodies of each thematic map, between 2008 and 2015 of the semi-arid region. This is an important analysis when planning multiple water uses.

The linear regression mathematical model highlights the existence of a functional relation between the areas with “water bodies x imaging day”, with a coefficient of determination ( $R^2$ ) of 0.8794. On 09/21/2009, due to regular rain periods, the municipality had areas covered by water bodies of about 78.86 km<sup>2</sup> of the total area. However, with the drought intensification from 2012 onwards, the reservoir water condition tended to have an impacting reduction over

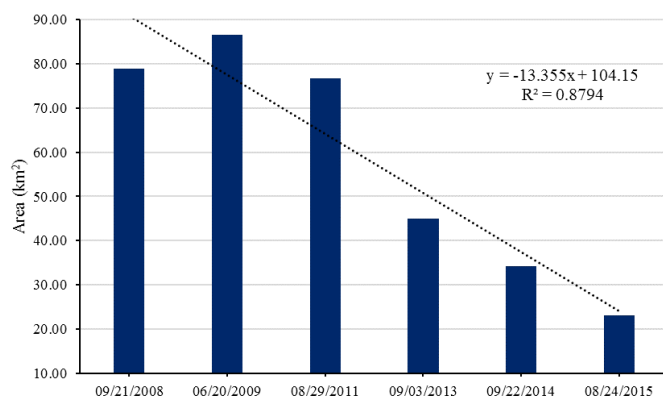


**Figure 4.** Quantification of areas covered by water bodies over time in the municipality of Iguatu-CE, semi-arid region from Northeastern Brazil.

time, as it is the case on 08/24/2015, with areas covered by water bodies of only 23.10 km<sup>2</sup> of the total area (Figure 4). In fact, the low reservoirs levels verified that the municipality faced severe drought and water scarcity conditions, which directly or indirectly affected multiple uses, such as human supply conditions, and in more remote areas, animal hydration was also affected, and even the main irrigated agriculture systems of the region.

Classes 3 and 4 highlight the distribution of areas of exposed soil, urban area and thin vegetation of Caatinga, having high percentages. In general, the region shows, due to the spatial-temporal analysis, a tendency of low vegetation cover, with mean values lower than 0.30 (Table 3), related to the variation of water availability that is mainly related to the dry season (period of images), which has a high water deficit (low soil moisture) over the semi-arid regions, causing changes and imminent decrease of the Caatinga vegetation leaf canopy, which explains, for the most part, the increase of values along time. During the dry period, the fall of deciduous leaves in deciduous plants, predominant in the Caatinga vegetation, is natural, as it is considered a condition of physiological defense of these plants, called leaf abscission, a typical phenomenon of this biome (Bezerra et al., 2014).

Undisciplined anthropogenic activities also contribute to the increase of exposed soil areas in the region, since it is common to practice deforestation and burning of Caatinga vegetation for agricultural purposes. At some points, in the southern region of the SAVI thematic maps (Figure 2), surrounded by red circles, there are pixels with similar spots that remained over time with SAVI values in the zero range, which indicates lower recovery capacity due to the deforestation of forest remnants, as well as other points in the region that deserve attention in order to avoid the occurrence of advanced environmental degradation processes.

It is worth mentioning that the vegetation cover responded proportionally to the events of previous rainfall, in other words, the higher/lower the rainfall was, the lower the Caatinga vegetation recovery capacity would be. In this sense, the thematic map of 06/20/2009 (Figure 2B) stands out,

**Table 3.** Statistical parameters and quantitative and spatial-temporal variability of SAVI and LAI vegetation indexes in the municipality of Iguatu-CE, semi-arid region of Northeastern Brazil.

Satellite	Date	Minimum	Maximum	Mean	Median	Mode	SD	CV (%)
Vegetation index – SAVI								
Landsat-5 TM	09/21/2008	-0.29	0.71	0.21	0.22	0.22	0.12	57
	06/20/2009	-0.71	0.84	0.47	0.55	0.59	0.20	42
	08/29/2011	-0.30	0.86	0.26	0.26	0.24	0.13	50
Landsat-8 OLI	09/03/2013	-0.43	0.81	0.25	0.28	0.26	0.12	48
	09/22/2014	-0.29	0.79	0.26	0.25	0.25	0.10	38
	08/24/2015	-0.37	0.83	0.26	0.26	0.25	0.09	35
Vegetation index – LAI (m <sup>2</sup> m <sup>-2</sup> )								
Landsat-5 TM	09/21/2008	0.0	5.98	0.28	0.24	0.22	0.25	89
	06/20/2009	0.0	6.00	1.55	1.60	0.50	0.98	63
	08/29/2011	0.0	5.97	0.41	0.34	0.25	0.30	73
Landsat-8 OLI	09/03/2013	0.0	6.00	0.48	0.41	0.34	0.42	87
	09/22/2014	0.0	6.00	0.40	0.34	0.31	0.31	77
	08/24/2015	0.0	6.00	0.41	0.34	0.31	0.43	104

where are observed a greater distribution of water body areas (classes 1 and 2) and a reduction of areas devoid of vegetation that showed resilience (classes 3 and 4), with values of 5.33% (54.83 km<sup>2</sup>) and 16.57% (170.40 km<sup>2</sup>), respectively (Figure 3).

At the same time, on 06/20/2009 (Figure 2B), there is a high regeneration of Caatinga and maintenance of dense and irrigated areas (classes 5 and 6), with percentages of 30.91% (317.88 km<sup>2</sup>) and 38.77% (398.75 km<sup>2</sup>), respectively (Figure 3). This behavior is directly associated with rainfall rates of the 30 previous days and of the previous trimester (Table 1) to the satellite passages, which allowed higher soil moisture and, consequently, the development of plant biomass. Thus, the denser Caatinga stood out in relation to the thinner Caatinga, which influenced the increase in SAVI. This corroborates the results of Bezerra et al. (2014), in research on biophysical parameters of the semi-arid region of Brazil through remote sensing, when they evaluated the vegetation index of normalized difference and found that the highest values were detected on the days that rain events occurred, which directly favored resilience of the native vegetation of Caatinga.

Arraes et al. (2012), when studying the dynamics of the energy balance on the Orós reservoir by remote sensing in the Alto Jaguaribe Basin, found the highest vegetation index values of the normalized difference in the imaging period that coincided with the end of the region rainy season, when, according to the authors, the striking presence of leaf canopy of Caatinga vegetation still concentrated on the areas of large herbaceous extract.

Caatinga vegetation is characterized by its high resilience, which enables the rapid formation of plant biomass soon after rain events, responsible for the accelerated response of energy and radiation balance components (Arraes et al., 2012; Bezerra et al., 2014).

Studies related to the Northeast Region and the territorial limits of the Brazilian semi-arid warn of the degradation worsening and greater susceptibility to desertification of areas due to the substitution of Caatinga natural environment in these regions by different land uses, considering factors such as inappropriate use and management mainly from agriculture, deforestation, forest burnings and extensive livestock (Vieira et al., 2013; Vieira et al., 2015).

According to data from MMA/IBAMA (2010), between 2002 and 2008, 40% of the total area of Caatinga was replaced by different land uses, highlighting that these landscape changes grow 0.3% per year. Vieira et al. (2015) while identifying areas susceptible to desertification in Northeastern Brazil also warned of an increase of about 3% of areas with high susceptibility over an 11-year period between 2000 and 2010.

Figure 5 displays the thematic maps of the spatial-temporal distribution of the LAI vegetation index between 2008 and 2015, which ranged from 0.0 to 6.00 m<sup>2</sup> m<sup>-2</sup>.

LAI vegetation index responded similarly to SAVI, showing the lowest values on water bodies, between 0.0 and 0.55 m<sup>2</sup> m<sup>-2</sup>. The areas of low vegetation cover, exposed soil and urban area had LAI values between 0.56 and 1.99 m<sup>2</sup> m<sup>-2</sup>. Areas of dense Caatinga and irrigated agriculture under conditions of

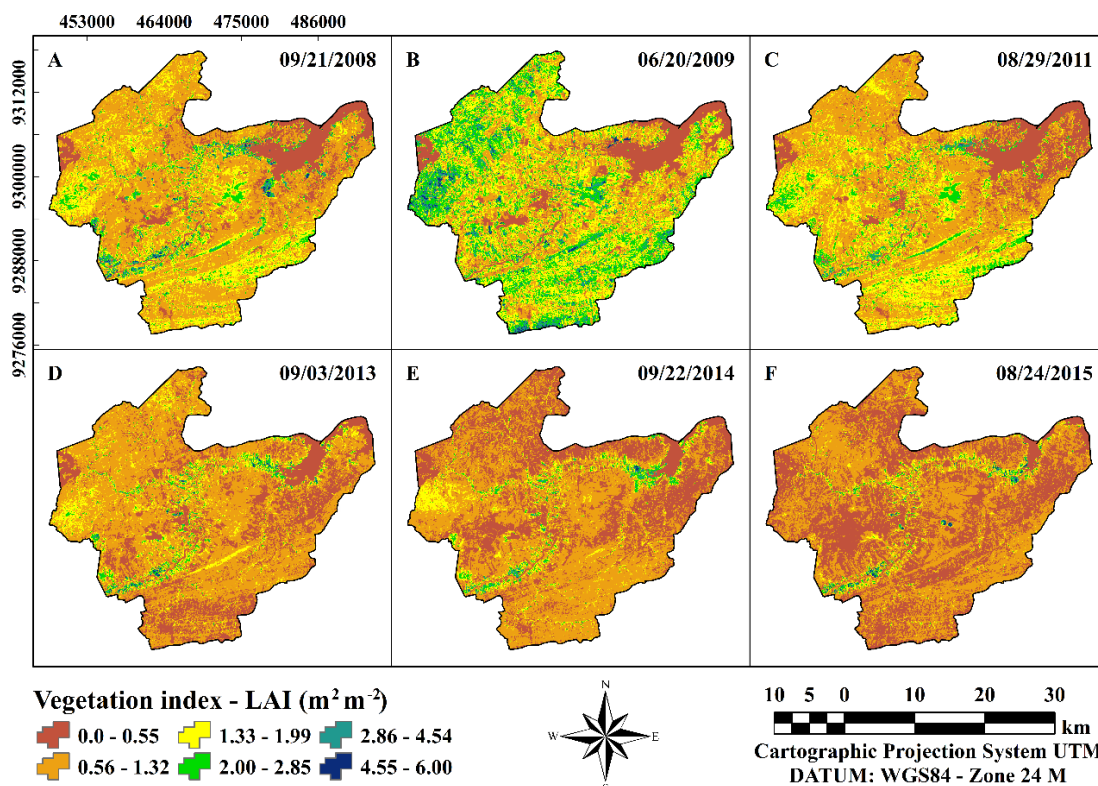


**Figure 5.** Spatial-temporal distribution of the LAI vegetation index in the municipality of Iguatu-CE, semi-arid region of Northeastern Brazil.

high soil moisture attained high values, reaching  $6.00 \text{ m}^2 \text{ m}^{-2}$  (Figure 5). LAI thematic maps indicated over time a similar behavior through the green pixels, showing high leaf mass near the water bodies, which are irrigated areas and remain photosynthetically active due to the presence of soil moisture (Figure 5).

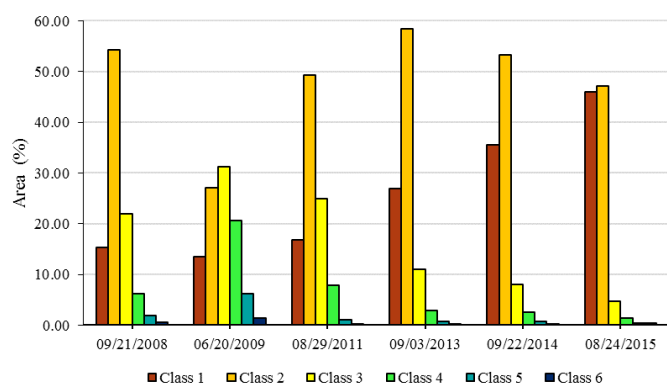
Barbosa et al. (2018), in a study on the Caatinga response to drought by vegetation index in the Brazilian semi-arid between 2008 and 2016, emphasized that Caatinga vegetation responds more strongly to rainfall events, emphasizing that the plants that have more deep roots and irrigated crops of deeper roots due to them being more resilient, are able to stay green even during drought, a condition that corroborates to the present study.

Figure 6 displays the quantification of areas according to the LAI index thematic map class ranges for the different land uses of the semi-arid region.

For the IAF, classes 1 and 2 represent the distribution of areas covered by water bodies, exposed soil, urban area and points with undergrowth. Classes 3; 4; 5 and 6 point out areas with vegetation cover, ranging from a thin and intermediate Caatinga to dense and irrigated areas with resilient and active vegetative power, mainly due to soil moisture (Figure 6).

Through the behavioral pattern of the temporal distribution of water bodies, this analysis also confirms the decrease in water mirrors, especially between 2013 and 2015, when drought periods directly affected the water condition of the region reservoirs, highlighting the days of 09/03/2013; 09/22/2014 and 08/24/2015, which obtained the increase of areas found by water reduction, with percentages of 26.90% ( $276.64 \text{ km}^2$ ); 35.50% ( $365.14 \text{ km}^2$ ) and 45.95% ( $472.60 \text{ km}^2$ ) of the total area, respectively (Figure 6).

As in SAVI, on 06/20/2009, the highest LAI values were observed (Table 3), a behavior related to the prior rainfall in greater depth, both in the 30 days (26 mm, Table 1) and in the previous trimester (516.2 mm, Table 1), with the image acquisition time being the transition period from the rainy



**Figure 6.** Quantification of the LAI thematic map class intervals in the different land uses and occupations of the semi-arid region. Class 1: between 0.0 and 0.55; Class 2: between 0.56 and 1.32; Class 3: between 1.33 and 1.99; Class 4: between 2.00 and 2.85; Class 5: between 2.86 and 4.54; Class 6: Between 4.55 and 6.00.

to the dry season, with a total annual precipitation (1,079.2 mm) above the historical mean of the municipality (817, 91 mm), which resulted in a greater balance between different land uses, as emphasized by the quantification of the classes in comparison to the other days (Figure 6). The larger events of previous rainfalls provided better water conditions to the rivers, lakes and reservoirs, reducing the negative effect of the accentuated water deficit, consequently resulting in better soil moisture conditions and imposing greater recovery and development of Caatinga vegetation, with rapid formation of leaf canopy and plant biomass (Figure 6). Arraes et al. (2012) stated that the temporal distribution of rainfall precipitations is one of the main factors to be considered in the natural environment of Caatinga, due to the strong influence on water balance and, consequently, on the soil moisture in the region.

Campos et al. (2019), in a study on the energy balance of a preserved area with Caatinga vegetation in the Brazilian semi-arid, pointed out that during the rainy season the NDVI vegetation index reached a maximum value of 0.80, due to the greater carbon assimilation by the plants. and increased vegetation productivity. However, in the dry season, when occurs the falling of leaves and loss of leaf canopy, a common defense mechanism of Caatinga vegetation, NDVI was reduced to 0.30, in response to the marked water deficit of the region, which automatically favors the reduction of photosynthetic activities.

The quantitative and spatial-temporal analysis of the SAVI and LAI indexes confirmed, based on their mean values of 0.21 to 0.47  $\text{m}^2 \text{ m}^{-2}$ , and from 0.28 to 1.55  $\text{m}^2 \text{ m}^{-2}$ , the vegetation low vigor (Table 3), characteristic of Caatinga in the dry season, when there is a reduction in plant biomass. Areas disproved of vegetation are highly vulnerable, as the water deficit and lack of soil moisture in conjunction with the high temperatures observed in the region may result in increased risk of environmental degradation and following desertification.

OLA/LAPIS (2019) researchers evaluated, through orbital remote sensing, the ecological resilience of Caatinga vegetation in the Brazilian semi-arid, between 2010 and 2016, to extreme weather events and pointed out that even under water availability conditions in view of rainfall, vegetation was less resilient due to deforestation, which significantly affected plant biomass productivity. Thus, in the present study, deforestation of forest remnants may also have possibly contributed to the increase of exposed soil areas, directly influencing energy exchanges between the earth surface and the atmosphere.

Silva & Galvncio (2012), in a study using remote sensing in the Brazilian semi-arid analyzing vegetation indexes, highlighted that SAVI has high accuracy in evaluating Caatinga vegetation, especially in the dry season of semi-arid regions, confirming in this study its high applicability and reliability of results.

Spatial-temporal distribution of the SAVI and LAI vegetation indexes, together with the quantification and characterization of these results for the Iguatu-CE region, demonstrate to be an effective part of an important environmental monitoring



for planning and management in the taking of measures and decisions environmental impact assessment, both in the municipality under analysis and in other regions of the Brazilian semi-arid.

## Conclusions

Quantitative and spatial-temporal analysis of the SAVI and LAI vegetation indexes showed low values of Caatinga plant biomass and leaf area, a characteristic behavior pattern of the Brazilian semi-arid, influenced by the dry season and low precipitation indexes.

SAVI and LAI temporal distribution patterns corresponded to the previous rainfall events, pointing out the Caatinga high resilience due to the rapid formation of plant biomass.

Spatial-temporal monitoring of Caatinga vegetation by means of vegetation indexes, in the development of thematic maps of the surface, originated responses of the behavioral pattern from the different land uses of the semi-arid region of Iguatu-CE, shedding light to the changing conditions and recovery capacity of the vegetation over time in the absence and/or presence of rain.

Remote sensing allowed the identification of quantitative variability and spatial-temporal monitoring of vegetative drought in Caatinga through vegetation indexes, detecting changes in the terrestrial surface that were more vulnerable, mainly due to the intensification of drought events in the semi-arid region.

## Acknowledgements

To the Federal Rural University of Pernambuco; Postgraduate Program in Agricultural Engineering. This study was conducted with the support of the Coordination for the Improvement of Higher Education Personnel - Brazil (CAPES) - Finance Code 001. The authors thank the National Council for Scientific and Technological Development (CNPq); NASA/USGS for providing satellite images; and INMET and ANA for providing surface data. The authors would like to thank the anonymous reviewers who read the manuscript and made essential observations and comments to improve the research.

## Literature Cited

- Allen, R.G.; Tasumi, M.; Trezza, R. Satellite-based energy balance for mapping evapotranspiration with internalized calibration (METRIC) – model. *Journal of Irrigation and Drainage Engineering*, v.133, n.4, p.380-394, 2007. [https://doi.org/10.1061/\(ASCE\)0733-9437\(2007\)133:4\(380\)](https://doi.org/10.1061/(ASCE)0733-9437(2007)133:4(380)).
- Allen, R.G.; Tasumi, M.; Trezza, R.; Bastiaanssen, W.G.M. SEBAL (Surface energy balance algorithms for land). *Advance training and users manual - Idaho Implementation, version 1.0*, 2002.
- Alvares, C.A.; Stape, J.L.; Sentelhas, P.C.; Moraes, G.; Leonardo, J.; Sparovek, G. Köppen's climate classification map for Brazil. *Meteorologische Zeitschrift*, v.22, n.6, p.711-728, 2013. <https://doi.org/10.1127/0941-2948/2013/0507>.
- Arraes, F.D.D.; Andrade, E.M.; Silva, B.B. Dinâmica do balanço de energia sobre o açude Orós e suas adjacências. *Revista Caatinga*, v.25, n.1, p.119-127, 2012. <https://periodicos.ufersa.edu.br/index.php/caatinga/article/view/2024/pdf>. 17 Mai. 2019.
- Barbosa, H.A.; Lakshmi Kumar, T.; Paredes, F.; Elliott, S.; Ayuga, J.G. Assessment of Caatinga response to drought using Meteosat-SEVIRI Normalized Difference Vegetation Index (2008–2016). *ISPRS Journal of Photogrammetry and Remote Sensing*, v.148, p.235-252, 2018. <https://doi.org/10.1016/j.isprsjprs.2018.12.014>.
- Bastiaanssen, W.G.M. SEBAL-based sensible and latent heat fluxes in the irrigated Gediz Basin, Turkey. *Journal of Hydrology*, v.229, n.1-2, p.87-100, 2000. [https://doi.org/10.1016/S0022-1694\(99\)00202-4](https://doi.org/10.1016/S0022-1694(99)00202-4).
- Bezerra, J.M.; Moura, G.B.A.; Silva, B.B.; Lopes, P.M.O.; Silva, E.F.F. Parâmetros biofísicos obtidos por sensoriamento remoto em região semiárida do estado do Rio Grande do Norte, Brasil. *Revista Brasileira de Engenharia Agrícola e Ambiental*, v.18, n.1, p.73-84, 2014. <https://doi.org/10.1590/S1415-43662014000100010>.
- Campos, S.; Mendes, K. R.; Silva, L.L.; Mutti, P.R.; Medeiros, S.S.; Amorim, L.B.; Santos, C.A.C.; Perez-Marin, A.M.; Ramos, T.M.; Marques, T.V.; Lucio, P.S.; Costa, G.B.; Silva, C.M.S.; Bezerra, B.G. Closure and partitioning of the energy balance in a preserved area of a Brazilian seasonally dry tropical forest. *Agricultural and Forest Meteorology*, v.271, p.398-412, 2019. <https://doi.org/10.1016/j.agrformet.2019.03.018>.
- Chander, G.; Markham, B.L.; Helder, D. L. Summary of current radiometric calibration coefficients for Landsat MSS, TM, ETM+, and EO-1 ALI sensors. *Remote Sensing of Environment*, v.113, n.5, p.893-903, 2009. <https://doi.org/10.1016/j.rse.2009.01.007>.
- Gutiérrez, A.P.A.; Engle, N.L.; De Nys, E.; Molejón, C.; Martins, E.S. Drought preparedness in Brazil. *Weather and Climate Extremes*, v.3, p.95-106, 2014. <https://doi.org/10.1016/j.wace.2013.12.001>.
- Huete, A.R. A soil adjusted vegetation index (SAVI). *Remote Sensing of Environment*, v.25, n.3, p.295-309, 1988. [https://doi.org/10.1016/0034-4257\(88\)90106-X](https://doi.org/10.1016/0034-4257(88)90106-X).
- Instituto Nacional de Meteorologia - INMET. Estação Meteorológica de observação de superfície automática. <http://www.inmet.gov.br/portal/index.php?=estacoes/estacoesAutomaticas>. 08 Abr. 2019.
- Instituto de Pesquisa e Estratégia Econômica do Ceará - IPECE. Perfil municipal 2017 - Iguatu. Fortaleza: IPECE, 2017. 18p. [https://www.ipece.ce.gov.br/wp-content/uploads/sites/45/2018/09/Iguatu\\_2017.pdf](https://www.ipece.ce.gov.br/wp-content/uploads/sites/45/2018/09/Iguatu_2017.pdf). 17 Abr. 2019.
- Iqbal, M. An introduction to solar radiation. London: Academic Press., 1983. 390p.
- Leite, A.P.; Santos, G.R.; Santos, J.É.O. Análise temporal dos índices de vegetação NDVI e SAVI na Estação Experimental de Itatinga utilizando imagens Landsat 8. *Revista Brasileira de Energias Renováveis*, v.6, n.4, p.606-623, 2017. <https://doi.org/10.5380/rber.v6i4.45830>.
- Lins, F.A.C.; Araújo, D.C.S.; Silva, J.L.B.; Lopes, P.M.O.; Oliveira, J.D.A.; Silva, A.T.G.C.S.G. Estimativa de parâmetros biofísicos e evapotranspiração real no semiárido Pernambucano utilizando sensoriamento remoto. *Irriga*, v.1, n.1, p.64-75, 2017. <https://doi.org/10.15809/irriga.2017v1n1p64-75>.

- Maranhão, D.D.C.; Pereira, M.G.; Costa, E.M.; Anjos, L.H.C. Correção de imagens e caracterização do uso da terra no município de pinheiral, Estado do Rio de Janeiro, Brasil. *Caminhos de Geografia*, v.18, n.62, p.174-178, 2017. <http://www.seer.ufu.br/index.php/caminhosdegeografia/article/view/36893/20587>. 01 Abr. 2019.
- Marengo, J.A.; Alves, L.M.; Alvalá, R.; Cunha, A.P.; Brito, S.; Moraes, O.L. Climatic characteristics of the 2010-2016 drought in the semiarid Northeast Brazil region. *Anais da Academia Brasileira de Ciências*, v.90, n.2, supl. 1. p.1973-1985, 2018. <https://doi.org/10.1590/0001-3765201720170206>.
- Marengo, J.A.; Torres, R.R.; Alves, L.M. Drought in Northeast Brazil-past, present, and future. *Theoretical and Applied Climatology*, v.129, n.3-4, p.1189-1200, 2016. <https://doi.org/10.1007/s00704-016-1840-8>.
- Mariano, D.A.; Santos, C.A.; Wardlow, B.D.; Anderson, M.C.; Schiltmeyer, A.V.; Tadesse, T.; Svoboda, M.D. Use of remote sensing indicators to assess effects of drought and human-induced land degradation on ecosystem health in Northeastern Brazil. *Remote Sensing of Environment*, v.213, p.129-143, 2018. <https://doi.org/10.1016/j.rse.2018.04.048>.
- Ministério do Meio Ambiente; Instituto Brasileiro do Meio Ambiente e dos Recursos Naturais Renováveis - MMA/IBAMA. Monitoramento dos desmatamentos nos biomas brasileiros por satélite - Monitoramento do bioma Caatinga: 2002 a 2008. Brasília: MMA; IBAMA, 2010. 58p. [http://www.mma.gov.br/estruturas/sbf\\_chm\\_rbbio/\\_arquivos/relatrio\\_tcnico\\_caatinga\\_72.pdf](http://www.mma.gov.br/estruturas/sbf_chm_rbbio/_arquivos/relatrio_tcnico_caatinga_72.pdf). 30 Abr. 2019.
- Organização Letras Ambientais; Laboratório de Análise e Processamento de Imagens de Satélites - OLA/LAPIS. Caatinga: um dos biomas menos protegidos do Brasil. [https://www.letrasambientais.com.br/posts/caatinga:-um-dos-biomas-menos-protegidos-do-brasil?fbclid=IwAR2XZ1wmav3Z9i-MEt4wSbFoPDzLLTWeuMy50auzxpbrLTgX34L\\_yz1cGvs](https://www.letrasambientais.com.br/posts/caatinga:-um-dos-biomas-menos-protegidos-do-brasil?fbclid=IwAR2XZ1wmav3Z9i-MEt4wSbFoPDzLLTWeuMy50auzxpbrLTgX34L_yz1cGvs). 30 Abr. 2019.
- Oliveira, J.D.A.; Medeiros, B.C.; Silva, J.L.B.; Moura, G.B.A.; Lins, F.A.C.; Nascimento, C.R.; Lopes, P.M.O. Space-temporal evaluation of biophysical parameters in the High Ipanema watershed by remote sensing. *Journal of Hyperspectral Remote Sensing*, v.7, n.6, p.357-366, 2017. <https://periodicos.ufpe.br/revistas/jhrs/article/view/230865/27949>. 27 Jul. 2019.
- Ribeiro, E.P.; Nóbrega, R.S.; Mota Filho, F.O.; Moreira, E.B. Estimativa dos índices de vegetação na detecção de mudanças ambientais na bacia hidrográfica do rio Pajeú. *Geosul*, v.31, n.62, p.59-92, 2016. <https://doi.org/10.5007/2177-5230.2016v31n62p59>.
- Silva, L.G.; Galvíncio, J.D. Análise comparativa da variação nos índices NDVI e SAVI no Sítio PELD – 22, em Petrolina – PE, na primeira década do século XXI. *Revista Brasileira de Geografia Física*, v.5, n.6, p.1446-1456, 2012. <https://periodicos.ufpe.br/revistas/rbgfe/article/view/232936/26908>. 25 Mar. 2019.
- Vieira, R.M.S.P.; Cunha, A.P.M.A.; Alvalá, R.C.S.; Carvalho, V.C.; Ferraz Neto, S.; Sestini, M.F. Land use and land cover map of a semi-arid Region of Brazil for meteorological and climatic models. *Revista Brasileira de Meteorologia*, v.28, n.2, p.129-138, 2013. <https://doi.org/10.1590/S0102-77862013000200002>.
- Vieira, R.M.S.P.; Tomasella, J.; Alvalá, R.C.S.; Sestini, M.F.; Affonso, A.G.; Rodriguez, D.A.; Barbosa, A.A.; Cunha, A.P.M.A.; Valles, G.F.; Crepani, E.; Oliveira, S.B.P.; Souza, M.S.B.; Clili, P.M.; Carvalho, M.A.; Valeriano, D.M.; Campello, F.B.; Santana, M.O. Identifying areas susceptible to desertification in the Brazilian northeast. *Solid Earth*, v.6, n.1, p.347-360, 2015. <https://doi.org/10.5194/se-6-347-2015>.
- Warrick, A.W.; Nielsen, D.R. Spatial variability of soil physical properties in the field. In: Hillel, D. (Ed.). *Applications of soil physics*. New York: Academic Press, 1980. p.319-344.